DOI: 10.3901/CJME.2016.0129.017, available online at www.springerlink.com; www.cjmenet.com

Non-Contact Electromagnetic Exciter Design with Linear Control Method

WANG Lin[1, *], XIONG Xianzhi[2], and XU Hua[3]

1 *School of Mechanical Engineering, Northwestern Polytechnical University, Xi'an 710072, China*
2 *Xi'an High Voltage Apparatus Research Institute Co., Ltd, Xi'an 710077, China*
3 *Key Laboratory of Education Ministry for Modern Design and Rotor-Bearing System, Xi'an Jiaotong University, Xi'an 710049, China*

Received October 14, 2015; revised December 23, 2015; accepted January 29, 2016

Abstract: A non-contact type force actuator is necessary for studying the dynamic performance of a high-speed spindle system owing to its high-speed operating conditions. A non-contact electromagnetic exciter is designed for identifying the dynamic coefficients of journal bearings in high-speed grinding spindles. A linear force control method is developed based on PID controller. The influence of amplitude and frequency of current, misalignment and rotational speed on magnetic field and excitation force is investigated based on two-dimensional finite element analysis. The electromagnetic excitation force is measured with the auxiliary coils and calibrated by load cells. The design is validated by the experimental results. Theoretical and experimental investigations show that the proposed design can accurately generate linear excitation force with sufficiently large amplitude and higher signal to noise ratio. Moreover, the fluctuations in force amplitude are reduced to a greater extent with the designed linear control method even when the air gap changes due to the rotor vibration at high-speed conditions. Besides, it is possible to apply various types of excitations: constant, synchronous, and non-synchronous excitation forces based on the proposed linear control method. This exciter can be used as linear-force exciting and controlling system for dynamic performance study of different high-speed rotor-bearing systems.

Keywords: non-contact excitation, electromagnetic exciter, journal bearing, finite element analysis

1 Introduction

Embedded motorized spindles are key components of high-speed grinding machine tools. Dynamic performance of the machine tools is greatly influenced by stability of the high-speed spindles[1]. Reliability and stability of the spindles has become a major concern with the increased operating speed and load. Further, dynamic performance of the spindles and the machine tools is partially determinied by the supporting bearings. Jounal bearings as support mechanism for high-speed grinding spindles have multiple advantages, such as low maintenance cost, high reliability, and long lifetime[2–3]. Besides, they also provide a positive damping between rotor and stator to minimize resonance effects. Accurate prediction of the bearing dynamic coefficients in actual operating conditions is necessary for the design and operation of machines tools. Thus, experimental identification of the bearing dynamic coefficients is vital for a good understanding of dynamic performance in high-speed spindle systems[4]. However, it is difficult to investigate the dynamic performance of high-speed rotor-bearing systems experimentally owing to its high-speed and complicated running conditions.

Experiments on high-speed journal bearings are complex mainly because of excitation system design that needs to provide broad frequency and displacement range, and collecting force and displacement data. The bearing dynamic coefficients can be identified by using inverse method, where the rotor is held rigidly while exciting the moving bearing housing[5–7]. However, in the real operating conditions, the bearing housing is held rigidly with a rotating rotor. In this case, the exciting force has to be applied on the moving rotor, so the use of non-contact type force actuators to excite the rotor-bearing system is necessary, especially for high-speed working conditions.

To accurately evaluate and further improve the performance of high-speed spindles, it is necessary to develop an efficient technique to investigate the dynamic coefficients of high-speed bearings under different operating conditions.

The non-contact type force actuators have been proposed recently to control the rotor-bearing system where the actuators are typically active magnetic bearings(AMB) or non-contact electromagnetic shakers. The shaft of rotating machinery will be supported and excited by a non-contact type force actuators simultaneously[8–11]. Such actuators

* Corresponding author. E-mail: wanglin@nwpu.edu.cn

Supported by National Natural Science Foundation of China(Grant Nos. 51505384, 51575421), Fundamental Research Funds for the Central Universities, China(Grant No. 3102015JCS05007), and Aeronautical Science Foundation of China(Grant No. 20140453008)

allow flexibility in the applied force, so either the sinusoidal, unidirectional, or pseudorandom excitation can be applied on the rotor[12–14]. KNOPF and NORDMANN[15] used magnetic bearings as actuators to identify the bearing coefficients of turbulent plain journal bearings. A stepped sine forcing function was applied to the bearing non-synchronously. KIM and LEE[16] proposed an AMB excitation system and experimentally identified the dynamic coefficients of an oil-lubricated and short squeeze film damper. BELLABARBA, et al[17], used AMB as force exciters to identify dynamic coefficients for air bearings. The rotor was supported with two magnetic bearings, with the test air bearing in the center. ZUTAVERN and CHILDS[18] applied dynamic loads to excite a flexible rotor system supported by magnetic bearings. Stiffness and damping coefficients of an annular gas seal were determined using a frequency domain method. MA, et al[19], developed a novel structure similar with magnetic bearings as the active online balancing devices, and the feasibility of this new type of balancing device was verified by experiments.

The above experiments using AMB (or similar structure) as actuators provides the flexibility to select arbitrarily the static operating position of the journal with different values of clearance, contact-free excitation, arbitrary manipulation of excitation amplitude, phase and frequency and simulate various situations which might occur in a rotor-bearing system.

The structure of non-contact electromagnetic exciters is simpler than the AMB, but only act as force exciters for shaft of rotating machinery[20–21]. ARUMUGAM, et al[22], identified the stiffness and damping coefficients of the tilting pad and cylindrical journal bearings of a flexible rotor-bearing system using a non-contact electromagnetic exciter. Frequency response functions were obtained from the experimental measurements and the finite element method, and bearing coefficients were calculated with a least squares method. REDDY, et al[23], investigated the stiffness and damping coefficients of tilting pad journal bearings with small L/ D ratios using the non-contact electromagnetic exciter method. The experimentally identified coefficients showed a good agreement with the theoretically calculated values for different L/D ratios. BEDIZ, et al[24–25], designed a electromagnetic exciter for model testing of miniature high-speed spindles.

However, the non-contact exciters that are currently available either have relatively complex structures that creates difficulty while applying different forces or limited by high power loss, limited amplitude and excitation frequency range under high speed conditions. Besides, variation in the air gap increases with the rotating speed owing to the rotor vibration, while the non-linear electromagnetic force is sensitive to the air gap thickness and current. So a linear force is necessary to apply especially at high-speed operation conditions.

In this paper, a simple non-contact electromagnetic exciter for studying the dynamic performance of high-speed journal bearings is designed. The non-contact electromagnetic exciter can linearly generate a more adjustable excitation force with a larger force amplitude and a higher signal to noise ratio. The exciter can be easily extended to impact rotors with different diameters by adjusting the structure of the armature. Analytical models based on the finite element method(FEM) are developed to investigate the factors that influences the exerted electromagnetic force, such as current amplitude, armature misalignment, excitation frequency, and rotating speed. Then the force is measured with auxiliary coils for subsequent journal bearing dynamic tests.

2 Structure and Principle

The non-contact electromagnetic exciting system with adjustable force directions consists of an electromagnetic exciter, one computer, two AD conversion modules, two power amplifiers, two diode shunt circuits, two load cells (2), etc., and schematic of such exciter system is shown in Fig. 1. The electromagnetic exciter contains four U-shaped iron cores(4a–4d), four coil windings(5a–5d), and an armature(7) fixed on the spindle(8). The iron cores are independently fixed between two stainless and diamagnetic steel plates(3) as shown in Fig. 2.

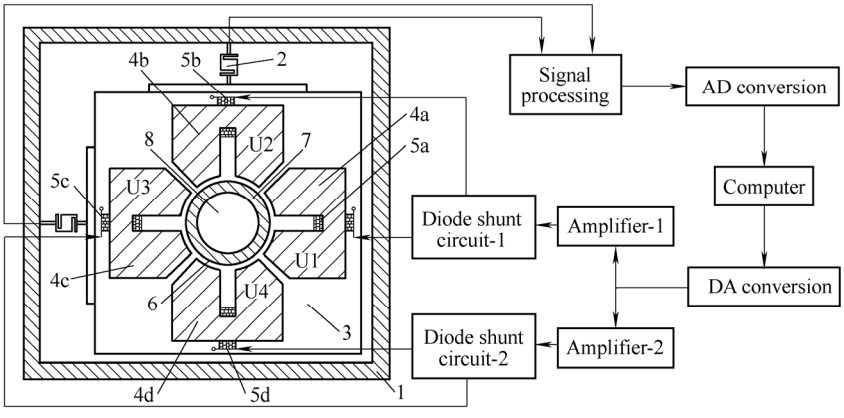

Fig. 1.　Schematic of the non-contact electromagnetic exciting system

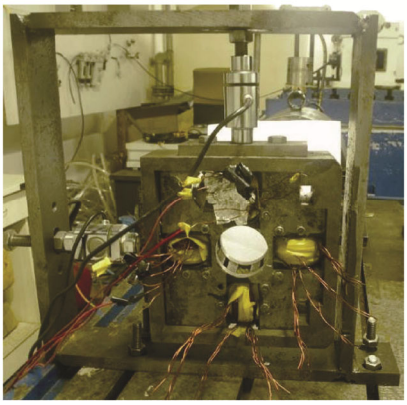

(a) Front view

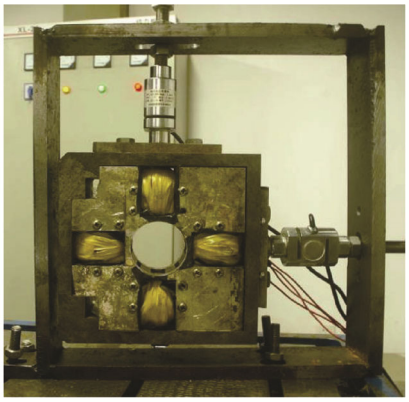

(b) Back view

Fig. 2. General view of the exciter

The signal processing component, the AD conversion component, the DA conversion component, and the PID controller are integrated on a PXI data acquisition equipment, which is connected with the computer.

The force in the electromagnetic bearings can be calculated by the following equation:

$$F=\frac{\phi^2}{2K_f^2\mu_0 S}=\frac{\mu_0 S(NI)^2}{2K_f^2\sigma^2}, \tag{1}$$

where μ_0 is the magnetic permeability of air, S is the area of the air gap, N is the number of turns in the coil, I is the alternating input current, K_f is the leakage coefficient, σ is the air gap thickness.

It can be seen that the non-linear electromagnetic force is proportional to the square of alternating input current and is sensitive to any variations in the input current and air gap thickness. So an approximated linear force transformation is necessary.

Flow chart for the proposed linear force control method is shown in Fig. 3. F_x and F_y are the expected sinusoidal excitation forces, and are determined by the input current in the coil windings. R_x and R_y are square root of R_x and R_y respectively. F_{xm} and F_{ym} are the electromagnetic force measured by the auxiliary coils, while R_{xm} and R_{ym} are the square root of F_{xm} and F_{ym} respectively. The feedback to the PID controller is R_{xm} and R_{ym}, while the inputs are R_x and R_y. Output of the PID controller is in the form of digital value, which is converted into an appropriate control voltage after DA conversion. Then the control voltage is amplified by the power amplifiers and changed into current of the coil windings in the electromagnetic exciter. The diode shunt circuits are based on the unidirectional conductivity of the diodes, and are used to convert alternating current from the output of two power amplifiers into direct current, and then the direct current is used as the input current of four coil windings to generate expected sinusoidal excitation forces.

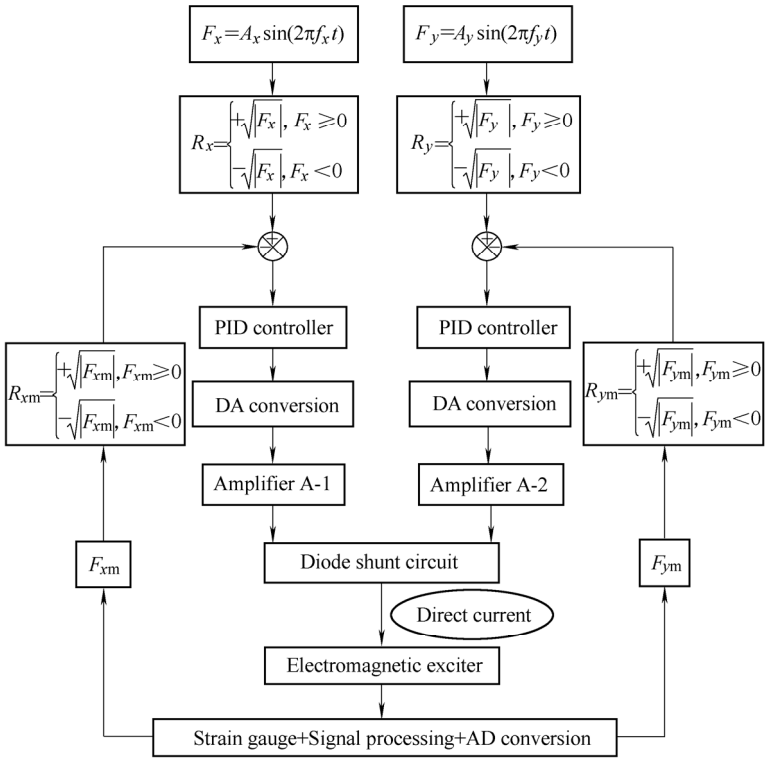

Fig. 3. Flow chart of linear force control method

Thus, the system controlled by the PID controller is changed into an easily adjustable linear force system, which can precisely control the linear excitation force.

The exciter consists of four independent excitation poles (U1–U4) arranged in horizontal and vertical directions, which is different with the electromagnetic bearing's integral structure. This structure is helpful for winding the coil, increasing the area and reduces the effective length of the magnetic circuit. The electromagnets U1 and U2 are controlled by the power amplifier A-1 and electromagnets U3 and U4 are controlled by the power amplifier A-2. If the expected electromagnetic force is positive, then input of the PID controller is the positive square root of the expected electromagnetic force, and vice-versa. Outputs of the PID controller and the power amplifier can have both positive and negative values. As the amplitude and direction of the electromagnetic force depend on the input current, so the diode shunt circuits are used to get the expected current directions as shown in Fig. 4. For example, when I_1 (or I_2) is positive, the current can pass through diode D_1 (or D_3), then electromagnet U1 (or U3) generates a horizontal force i.e., a force to the right (or left) direction; when I_1 (or I_2) is negative, the current can pass through diode D_2 (or D_4), then electromagnet U2 (or U4) generates a vertical force i.e., a force in the upward (or downward) direction. Only one excitation pole can generate electromagnetic force in horizontal or vertical directions at the same time.

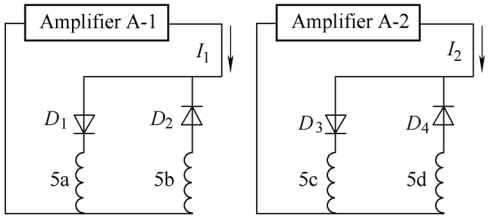

Fig. 4. Principle of diode shunt circuits

The magnetic coils are made of laminated silicon steel to reduce eddy current losses. The material of the armature is soft magnetic steel ASTM1045. Four magnetic coils are fixed between two stainless and diamagnetic steel plates after arranging windings on the cores. The coil windings are wound by using multiple parallel enameled wires.

All individual magnetic-flux lines are assumed to have equal length. Fringing effect, flux leakage, and magnetic hysteresis are assumed to be negligible. Besides, magnetic materials obey linear relationship between magnetic flux density(B) and the magnetic field intensity(H) within the material. All magnetic permeability is considered to be constant. Then the generated electromagnetic force between the pole of iron core and the armature is given as

$$F = \frac{B^2 S}{2\mu_0} = \frac{\mu_0 S(NI)^2}{8\sigma^2} = \frac{\mu_0 S(NI_c \cos \omega t)^2}{8\sigma^2} = \frac{1}{2} \bullet \frac{\mu_0 S(NI_c)^2}{8\sigma^2} + \frac{1}{2} \bullet \frac{\mu_0 S(NI_c)^2}{8\sigma^2} \cos 2\omega t, \quad (2)$$

where I_c is amplitude of the current through harmonic excitation portion, ω is the current frequency.

It can be observed that the electromagnetic force is proportional to the square of input current and without the bias current, so the current in the coil is set to alternating current to get a low distortion harmonic force. The above electromagnetic force consists of a constant force and an alternating force with a frequency twice of the current frequency. This method has a lower requirement for coaxiality of iron core and armature, so the influence of spindle vibration can be greatly reduced.

The electromagnets of AMB are constructed in one integral structure. When one general electromagnet is electrified, distribution of its magnetic-flux line is shown in Fig. 5(a). The effective electromagnetic force is concentrated at one pole, and the magnetic-flux leakage is very obvious. So in our design, four independent U-shaped magnetic cores are used for exciter and a small clearance exists between two cores. The magnetic field distribution of the exciter is shown in Fig. 5(b). The magnetic-flux leakage is very little, and every electrified pole generates electromagnetic force. It can be deduced that the effective force generated by an independent structure is almost twice compared to an integral structure for the same power loss and size.

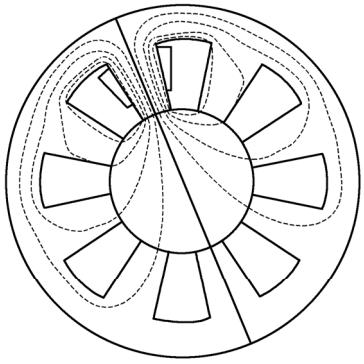

(a) General active magnetic bearing

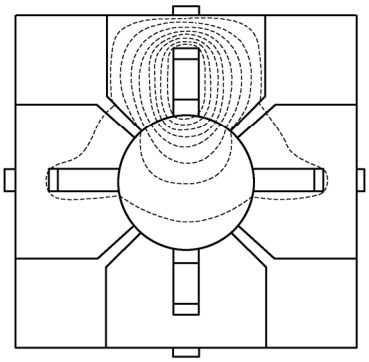

(b) Designed exciter

Fig. 5. Magnetic-flux line distribution

The excitation force should be able to excite appropriate vibration amplitude while should not induce the nonlinearity of bearing coefficients. The stiffness coefficients when estimated theoretically, they are of the

order of 1×10^8, so the maximum electromagnetic excitation force is set to 400 N.

The required excitation force decreases with the air gap, while a larger air gap is helpful to install the exciter and avoid the contact between the pole of iron core and the armature. On the other hand, the required ampere-turns to generate the same excitation force increase with the air gap, which will lead to a larger power loss and installation space. The predicted rotor vibration amplitude is about 10 μm, so the air gap is set to a relatively larger value of 0.75 mm to minimize the influence of variation on electromagnetic force. The maximum magnetic-flux density is chosen to be 1.2 T based on the B-H curves of core and armature material. Parameters of the designed exciter are listed in Table 1.

Table 1. Parameters of the designed exciter

Parameter	Value
Maximum force frequency f_{max} /Hz	100
Maximum current frequency f_{Fmax} /Hz	50
Axial length L_s/mm	18.8
Number of turn N	114
Single pole area S/mm^2	350
Maximum output voltage U_{max} /V	30

3 Factors Influencing the Electromagnetic Force

A two-dimensional analytical model is developed based on FEM to analyse the influence of current amplitude, misalignment, current frequency, and rotational speed on magnetic field and excitation force. The meshed-element model of the exciter is outlined in Fig. 6. A path with a length of 55 mm is defined along the gap between the pole of iron core and the armature.

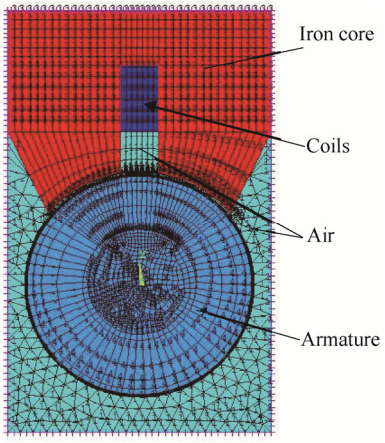

Fig. 6. Meshed-element model of the exciter

The influence of current variation on the electromagnetic force is analysed by the static magnetic analysis. Magnetic flux density distribution with a current of 12 A is shown in Fig. 7(a). It is found that the magnetic-flux density in the area closer to the position of the coil is much smaller than elsewhere, while the magnetic-flux density is nearly constant for other nodes of the path. So the exciter only generates normal force in the static current condition. As shown in Fig. 8(a), the electromagnetic force is linearly increasing with the square of current when the current is between 2 A and 12 A. However, the electromagnetic force increases slowly with the current when the current is between 12 A and 18 A. This is because the magnetic saturation becomes obvious and increases the magnetic resistance at higher currents.

The magnetic-flux density along the path with harmonic current presents a non-uniform distribution as shown in Fig. 7(b). The amplitude of the harmonic current is 12 A. The magnetic-flux density at the position of the coil area is still much smaller than elsewhere. However, the magnetic-flux density increases from both side of the pole to centre of the pole while reduces sharply at the edges of the coil area. The influence of current frequency on electromagnetic force is presented in Fig. 8(b). The force decreases with the current frequency. The average electromagnetic force in the harmonic current condition is only 42% of the static current condition when the current frequency is 50 Hz.

Misalignments between the armature and the pole surface of iron core are inevitable due to installation error and manufacturing imperfections, which will lead to the change in the air gap thickness and electromagnetic force. Fig. 7(c) and Fig. 8(c) present the influence of misalignment on the distribution of magnetic-flux density and electromagnetic force by the nonlinear static magnetic analysis. The misalignment is created by move the axis of armature away from the axis of iron core horizontally to the right. It can be seen that the misalignment leads to the asymmetricity and non-uniformness in the magnetic-flux density distributionand this asymmetry results in the generation of tangential electromagnetic force. Fig. 8(c) indicates that the normal and tangential electromagnetic force increase slowly with misalignment eccentricity ratio, and the ratio between the tangential and normal force also increases with the eccentricity ratio.

The influence of rotational speed on electromagnetic force is investigated using the harmonic analysis method. The amplitude of harmonic current is set to be a small value of 4 A to lower the influence of magnetic saturation. It can be seen from Fig. 7(d) that the magnetic flux density of two magnetic poles decreases along the rotation direction at a rotational speed of 30 000 r • min^{-1}. So the normal and tangential electromagnetic force generate simultaneously. Fig. 8(d) indicates that the normal electromagnetic force decreases while the tangential electromagnetic force slowly increases with the increase in rotational speed. And rate of this variation in both the cases slow down with the rotational speed. When the rotational speed is 30 000 r • min^{-1}, the normal force is only 48% of the static condition, and the ratio of the tangential and normal force is 1.8%.

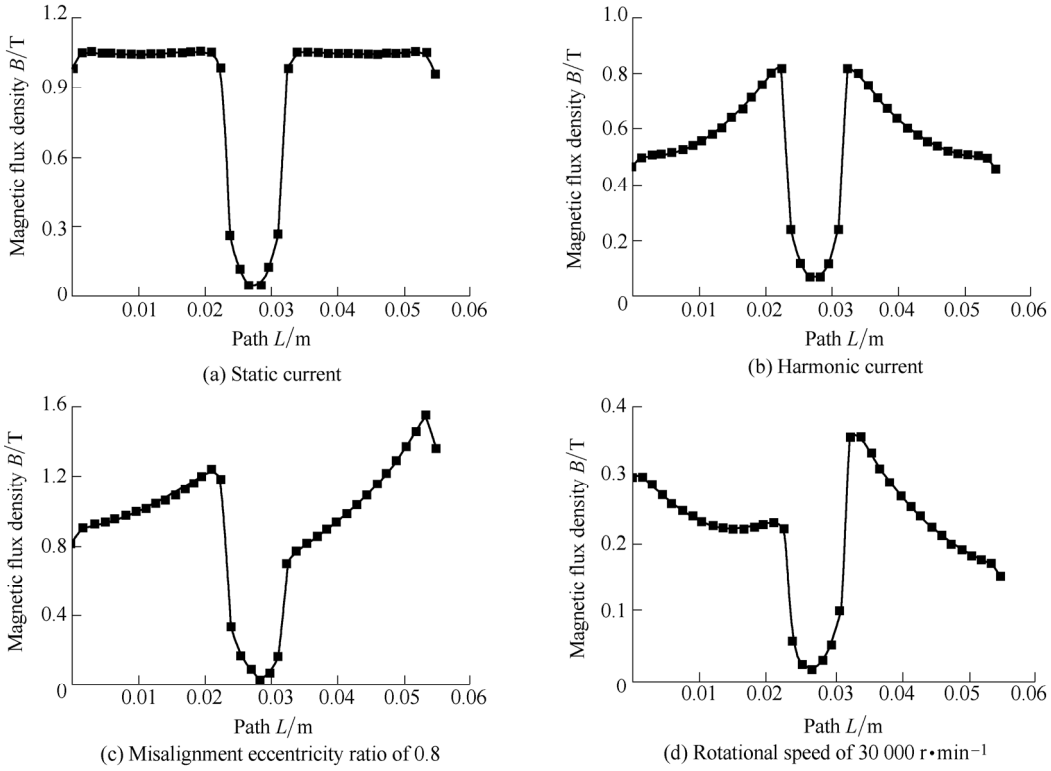

Fig. 7.　Distribution of magnetic-flux density along the path for different conditions

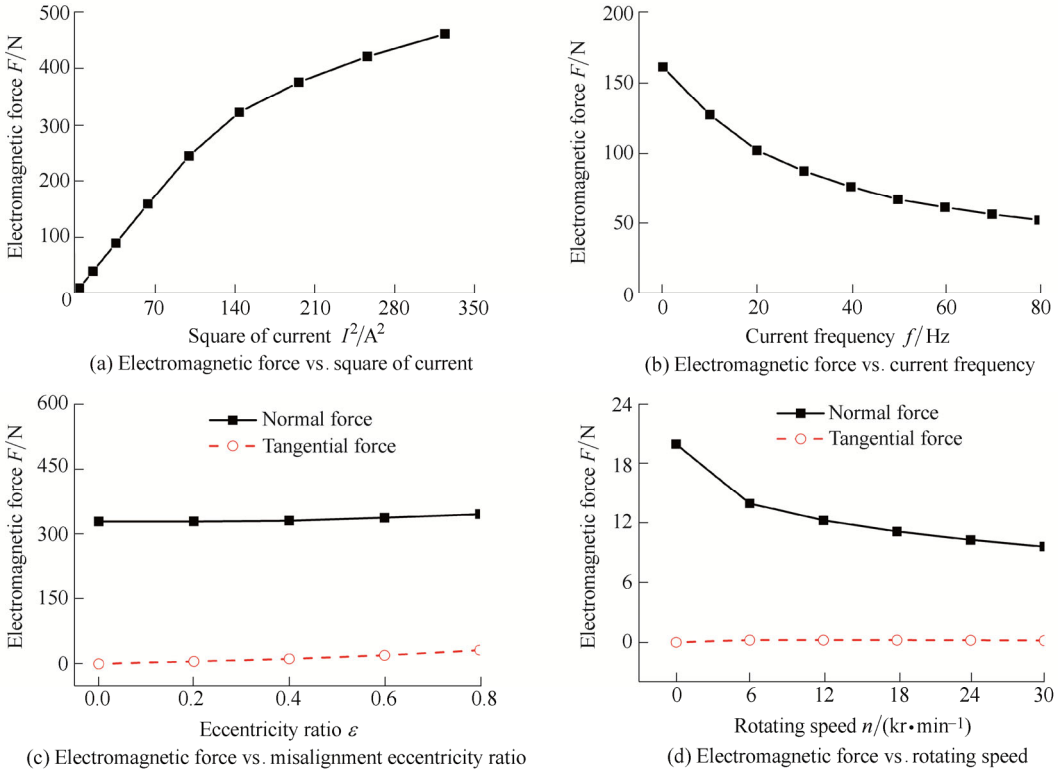

Fig. 8.　Electromagnetic force vs. the different parameters

4　Measurement and Calibration of the Electromagnetic Force

One of the challenges with the non-contact electromagnetic exciters is measuring the excitation force applied to the rotor-bearing system. A precise force measurement is also important for identifying the bearing dynamic coefficients. Electromagnetic forces are usually measured by strain gauges, piezoelectric load cells, magnetic flux sensors, and empirical current and position formulas[12, 15]. In this design, 30 turns of auxiliary coils are wounded around the field coils, and the electromagnetic

force can be obtained by converting the measured voltage of auxiliary coils.

The force measurement principle is briefly introduced here. The variations of the magnetic flux through the field coils will induce a voltage in the auxiliary coils, and then the electromagnetic force can be expressed by

$$F = \frac{B^2 S}{2u_0} = \frac{1}{2u_0 S N_{\mathrm{a}}^2}\left(\int e\mathrm{d}t\right)^2, \tag{3}$$

where N_{a} is the number of turns in the auxiliary coils, e is the induced voltage in the auxiliary coils.

Say, a current with the frequency ω flows through the field coils，then a voltage with the frequency ω will be induced in the auxiliary coils. The induced voltage can be expressed as

$$e = A_e \cos(\omega t + \theta), \tag{4}$$

where A_e is the amplitude of the induced voltage.

Substituting Eq. (3) into Eq. (2),

$$F = \frac{k_{fe}}{\omega^2}\left[1 + \cos(2\omega t + 2\theta + \pi)\right], \tag{5}$$

where $k_{fe} = \dfrac{A_e^2}{4u_0 S N_a^2}$.

The electromagnetic force consists of a static and a dynamic part. The dynamic part can be expressed by

$$F_d = A_f \cos(\omega t + \phi). \tag{6}$$

Then

$$A_f = \frac{k_{fe}}{\omega^2} A_e^2, \phi = 2\theta + \pi. \tag{7}$$

Hence the electromagnetic force can be obtained after determining k_{fe}.

Results presented in the previous section indicate that the magnetic-flux density is non-uniformly distributed in many cases. So it is necessary to evaluate how the distribution of the magnetic field affects the accuracy of the measured electromagnetic force. Fig. 9 is the outline of the iron core. L_{E1} and L_{E2} are the edges of two poles, and Z is the projection length of the pole in the horizontal direction.

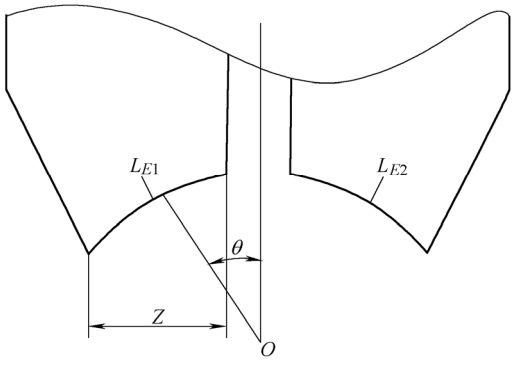

Fig. 9. Outline of the iron core

Magnetic flux density in the air gap is the function of position angle:

$$B = B(\theta). \tag{8}$$

The electromagnetic force in the non-uniform magnetic field can be expressed by

$$F_{\mathrm{nav}} = L_s \bullet \int_{L_{E1}+L_{E2}} \frac{B^2(\theta)}{2u_0}\mathrm{d}l\cos\theta. \tag{9}$$

However, in our actual experimental measurement by auxiliary coils, the magnetic flux density is assumed to be constant. Then the electromagnetic force in the uniform magnetic field can be expressed by

$$F_{\mathrm{av}} = 2 \bullet \frac{\overline{B}^2 Z L_{\mathrm{s}}}{2u_0}, \tag{10}$$

where $\overline{B}$ is equivalent magnetic flux density of the non-uniform magnetic field.

R_F is defined as the ratio of F_{nav} and F_{av}.

$$R_F = \frac{F_{\mathrm{nav}}}{F_{\mathrm{av}}}, \tag{11}$$

where F_{nav} and F_{av} are the electromagnetic forces in non-uniform and uniform magnetic field distribution cases respectively.

When R_F is close to one, it means that the magnetic field is more uniform and the measured force by auxiliary coils is more accurate. When R_F is greater than one, it means that the actual force is larger than the measured force, and vice-versa.

Values of R_F in different conditions mentioned in the above sections are calculated, and the maximum value is less than 1.1, which means that the accuracy of the measured force by auxiliary coils is acceptable.

The direct measurement of the electromagnetic force using an auxiliary coil can lower the influence of exciter vibration on frame, but the auxiliary coils need to be calibrated by load cells. Auxiliary coils are wounded on every electromagnet, and two load cells are respectively fixed in the horizontal and vertical directions. The top auxiliary coils are calibrated in the following.

To lower the influence of frame vibration on the load cell, the current frequency for calibration is 2.0 Hz. Fig. 10 indicates that the force amplitude A_f measured by the load cell increases linearly with the square of induced voltage A_e^2, especially when A_f is less than 30 N. The slope of this linear fitting curve, which is defined as R_{fe}, is 656.921 N/ V^2. To avoid the interaction between two load cells in orthogonal direction, the slope is computed for A_f less than 30 N case.

The measured force phase difference ($\Delta\theta$) between the load cell and auxiliary coils is shown in Fig. 11. The phase

difference is so small that its influence can be neglected.

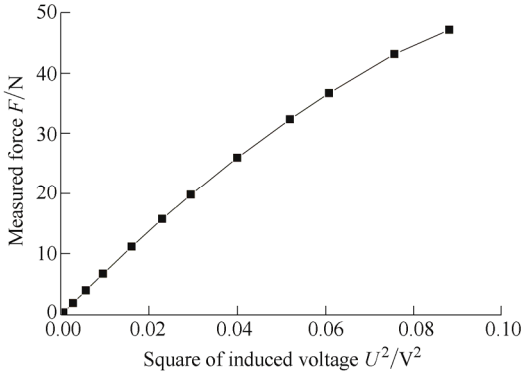

Fig. 10. Measured force vs. square of induced voltage

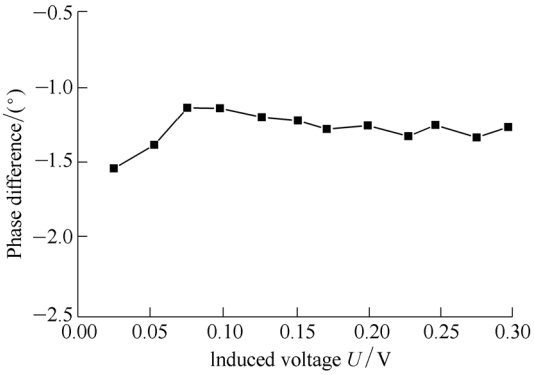

Fig. 11. Phase difference vs. induced voltage

Besides, a weight with a mass of 5.95 kg is used to calibrate the load cells. The weight is measured by the top load cell for three times. The average ratio R_{m} between the measured value and the actual mass is 0.889.

Hence the coefficient k_{fe} can be obtained by the following expression:

$$k_{fe}=\frac{R_{fe}\cdot R_m}{\omega^2}=\frac{656.92\times 0.889}{(2\times 2\pi)^2}=3.70.$$

5 Conclusions

(1) The proposed exciter has a linear adjustable excitation force, a larger force amplitude, and a higher signal to noise ratio for high-speed conditions;

(2) The exciter has a simple structure with four independent U-shaped electromagnets without using biased current;

(3) The exciter can be easily extended to other rotor-bearing systems with different diameters by adjusting the structure of the armature;

(4) A PID controller is used to adjust the excitation force, and make the exciter become a linear system, which is helpful for precisely controlling the excitation force in a wide range.

(5) The exciter can apply different constant, synchronous, and non-synchronous excitation forces based on the PID controller. This means that the exciter can be used for incremental loading excitation, sinusoidal excitation, transient excitation, or pseudorandom excitation.

(6) The designed non-contact electromagnetic exciter provide a simple and efficient linear-force exciting and controlling system for identifying bearing dynamic coefficients in high-speed journal bearings.

References

[1] MA Chi, MEI Xuesong, YANG Jun, et al. Thermal characteristics analysis and experimental study on the high-speed spindle system[J]. *International Journal of Advanced Manufacturing Technology*, 2015, 79(1–4): 469–489.

[2] WANG Lin, XU Hua. Experimental study on the dynamic performance of a new high-speed spindle supported by water-lubricated hybrid bearings[J/OL]. *Shock and Vibration*, 2016. doi: 10.1155/2016/8297834.

[3] ZHU Aibin, LI Pei, ZHANG Yefan, et al. Influence of particles on the loading capacity and the temperature rise of water film in Ultra-high speed hybrid bearing[J]. *Chinese Journal of Mechanical Engineering*, 2015, 28(3): 541–548.

[4] DIMOND T W, SHETH P N, ALLAIRE P E, et al. Identification methods and test results for tilting pad and fixed geometry journal bearing dynamic coefficients—A review[J]. *Shock and Vibration*, 2009, 16(1): 13–43.

[5] FRANCHEK N M, CHILDS D W, SAN ANDRES L. Theoretical and experimental comparisons for rotordynamic coefficients of a high-speed, high-pressure, orifice-compensated hybrid bearing[J]. *Journal of Tribology*, 1995, 117(2): 285–290.

[6] ZHAO Sanxing, ZHOU Hua, MENG Guang, et al. Experimental identification of linear oil-film coefficients using least-mean-square method in time domain[J]. *Journal of Sound and Vibration*, 2005, 287(4): 809–825.

[7] HONG Guo, XINMIN Lai, SHAOQI Cen. Theoretical and experimental study on dynamic coefficients and stability for a hydrostatic/hydrodynamic conical bearing[J]. *Journal of Tribology*, 2009, 131(4): 041701.

[8] BURROWS C R, KEOGH P S, SAHINKAYA M N. Progress towards smart rotating machinery through the use of active bearings[J]. *Proceedings of the Institution of Mechanical Engineers, Part C: Journal of Mechanical Engineering Science*, 2009, 223(12): 2849–2859.

[9] CADE I S, SAHINKAYA M N, BURROWS C R, et al. On the use of actively controlled auxiliary bearings in magnetic bearing systems[J]. *Journal of Engineering for Gas Turbines and Power*, 2009, 131(2): 022507.

[10] EL-SHAFEI A, DIMITRI A S. Controlling journal bearing instability using active magnetic bearings[J]. *Journal of Engineering for Gas Turbines and Power*, 2010, 132(1): 012502.

[11] QIU Ronghua, LIU Hongzhao. Non-contact dynamic electromagnetic loading on high speed motorized spindle[J]. *Journal of Vibration, Measurement & Diagnosis*, 2014, 34(2): 330–336. (in Chinese)

[12] FAN C C, PAN M C. Fluid-induced instability elimination of rotor-bearing system with an electromagnetic exciter[J]. *International Journal of Mechanical Sciences*, 2010, 52(4): 581–589.

[13] DAS A S, NIGHIL M C, DUTT J K, et al. Vibration control and stability analysis of rotor-shaft system with electromagnetic exciters[J]. *Mechanism and Machine Theory*, 2008, 43(10): 1295–1316.

[14] VIVEROS H P, NICOLETTI R. Lateral vibration attenuation of shafts supported by tilting-pad journal bearing with embedded electromagnetic actuators[J]. *Journal of Engineering for Gas Turbines and Power*, 2014, 136(4): 042503.

[15] KNOPF E, NORDMANN R. Identification of the dynamic characteristics of turbulent journal bearings using active magnetic bearings[C]//IMechE *Conference Transactions*, Professional Engineering Publishing, 1998, 2000, 6: 381–392.

[16] KIM K J, LEE C W. Identification of dynamic stiffness of squeeze film damper using active magnetic bearing system as an exciter[C]// *The 2nd International Symposium on Stability Control of Rotating Machinery(ISCORMA-2)*, 2003.

[17] BELLABARBA E, DÍAZ S, RASTELLI V. A test rig for air bearings rotordynamic coeffcients measurement[C]//*ASME Turbo Expo 2005: Power for Land, Sea, and Air*, American Society of Mechanical Engineers, 2005: 833–839.

[18] ZUTAVERN Z S, CHILDS D W. Identification of rotordynamic forces in a flexible rotor system using magnetic bearings[J]. *Journal of Engineering for Gas Turbines and Power*, 2008, 130(2): 022504.

[19] MA Shilei, PEI Shiyuan, WANG Lin, et al. A novel active online electromagnetic balancing method—principle and structure analysis[J]. *Journal of Vibration and Acoustics*, 2012, 134(3): 034503.

[20] KJØLHEDE K, SANTOS I F. Experimental contribution to high-precision characterization of magnetic forces in active magnetic bearings[J]. *Journal of Engineering for Gas Turbines and Power*, 2007, 129(2): 503–510.

[21] OUYANG Wu, ZHANG Fan, WANG Jianlei, et al. Research on magnetic loading in reliability enhancement testing of low viscosity lubricated bearings[J]. *Journal of Mechanical Engineering*, 2015, 51(4): 199–205. (in Chinese)

[22] ARUMUGAM P, SWARNAMANI S, PRABHU B S. Experimental identification of linearized oil film coefficients of cylindrical and tilting pad bearings[C]//*ASME 1994 International Gas Turbine and Aeroengine Congress and Exposition*. American Society of Mechanical Engineers, 1994: V005T14A012-V005T14A012.

[23] REDDY D S K, SWARNAMANI S, PRABHU B S. Experimental investigation on the performance characteristics of tilting pad journal bearings for small L/D ratios[J]. *Wear*, 1997, 212(1): 33–40.

[24] BEDIZ B, KORKMAZ E, BURAK OZDOGANLAR O. An impact excitation system for repeatable, high-bandwidth modal testing of miniature structures[J]. *Journal of Sound and Vibration*, 2014, 333(13): 2743–2761.

[25] BEDIZ B, GOZEN B A, KORKMAZ E, et al. Dynamics of ultra-high-speed(UHS) spindles used for micromachining[J]. *International Journal of Machine Tools and Manufacture*, 2014, 87: 27–38.

Biographical notes

WANG Lin, born in 1987, is currently an assistant research fellow at *School of Mechanical Engineering, Northwestern Polytechnical University, China*. He received his PhD degree from *Xi'an Jiaotong University, China*, in 2014. His research interests include tribology, rotor-bearing dynamics, and machinery science.
Tel: +86-29-88493929; E-mail: wanglin@nwpu.edu.cn

XIONG Xianzhi, born in 1989, is currently an engineer at *Xi'an High Voltage Apparatus Research Institute Co., Ltd, China*. He received his master's degree from *Xi'an Jiaotong University, China*, in 2014.
E-mail: xiongxianzhi@outlook.com

XU Hua, born in 1956, is currently a professor at *School of Mechanical Engineering, Xi'an Jiaotong University, China*. His research interests include tribology, rotor-bearing dynamics, and machinery science.
Tel: +86-29-82669157; E-mail: xuhua@mail.xjtu.edu.cn